Experiment Research on Cavitation Control by Active Injection

Shengpeng Lu[1]; *Wei Wang[1]; Tengfei Hou[1]; Mindi Zhang[2]; Jianxiong Jiao[1]; Qingdian Zhang[1]; Xiaofang Wang[1];

[1]*Key Laboratory of Ocean Energy Utilization and Energy Conservation of Ministry of Education, Dalian University of Technology, Dalian 116024, China*

[2]*School of Mechanical Engineering, Beijing Institute of Technology, Haidian district, Beijing, 100081, China*

Abstract

Based on the active control strategy of the flow, a method of suppressing cavitation by arranging water jet holes on the suction surface of the hydrofoil is proposed in this paper. The idea of cavitation control was tested in the experiments. The NACA0066 hydrofoil was placed in the test channel at an attack angle of 8°. The cavitation conditions were distinguished by cavitation number and the mass flow coefficient of the jet. High-speed flow field display technology was used to study the characteristics of cavitation. The influence of the jet mass flow on cavitation suppression was examined. The results show that the jet can suppress or weaken cavitation to an extent. With the decreasing of the cavitation number, the effect of the cavitation suppression was weakened, so the mass flow of the jet needed for cavitation suppressing was increased. And the optimum mass flow coefficient of the jet was obtained under different cavitation number.

Keywords: active control; cavitation; jet hole; jet flow; re-entrant jet

1 Introduction

It has been proved in the results of experiments [1-3] and numerical simulations [4-6] that the re-entrant jet and the lateral jet are the main reason for sheet cavitation changing into cloud cavitation. So, it can be started with suppressing the re-entrant jets or the lateral jets to suppress the transformation of sheet cavitation to cloud cavitation. At present, there are two main methods to suppress the re-entrant jets, which are based on different flow control strategies respectively. According to the different control methods, the flow control technology can be divided into active control technology and passive control technology. The active control technology is based on the input of external energy, and the control of flow is realized by coupling appropriate disturbance model with the internal flow model, such as injecting or inhaling a liquid [7-11], gas [12] or polymer solution [13] [14] through surface of the test object. Passive control doesn't require external energy input. It only changes the energy distribution of the fluid by passive devices to control the flow. It is worth noting that, for hydraulic machinery, its working conditions often changes. The passive control method [15] [16] (for example, the leading edge flap, vortex generator, hydrofoil surface modification, etc.) has a great influence on the hydrodynamic performance of the hydrofoil. And what's more important, once a certain passive device is applied to the surface of the test object, it is difficult to realize the interactive adjustment under different cavitation conditions. So, this paper pays more attention to the active flow control technology. Based on the active control strategy of the flow, a method of suppressing cavitation by arranging water jet holes on the surface of the hydrofoil is proposed. Through the design of the microstructures on the surface of the hydrofoil, the jet is ejected along the set channel to interfere with the re-entrants, and then the aim of suppressing cavitation is achieved. According to the degree of cavitation, by changing the flow rate of the jet, the momentum and velocity of the jet is adjusted, and thus the interactive adjustment under different cavitation conditions is realized. In the way of achieving the jet ejection by active flow control technology, the additional pump is used to pump the fluid into the cavity (which is set up in advance) of the hydrofoil, and then the fluid is ejected along the set flow channel. In the process, the velocity of the jet is regulated by adjusting the flowrate of the pump. The study of this paper is based on the analysis of the visual observations of cavities on side view, top view and oblique view gathered by high-speed imaging.

2 Experiments

2.1 Experiment Set up, object, control system and visualization techniques

*Corresponding Author, Wei Wang: wangw@dlut.edu.cn

All experimental study of this paper is carried out in cavitation tunnel. Its basic structure includes contraction, diffuser, experimental section, curved section, inlet pipe and return pipe, and upper and lower end are equipped with three high strength transparent organic glass windows to observe the flow field of water tunnel experiment section. The basic sizes of cavitation tunnel is listed in table 1.In the process of experiment, the dynamic system of tunnel is used to control and drive the water circulation in tunnel. Power system mainly includes a three-phase ac motor (1480 RPM, 55 kw), axial flow pump and control frequency converter. The cavitation tunnel is also equipped with a sliding precision protractor, electromagnetic flow meter (precision level 0.5%), torque device, vacuum head meter and other facilities. NACA0066 hydrofoil is adopted by the experiment which is made of stainless steel and the surface machining accuracy is 3.2 (microns), thickness ratio 11.74%, the hydrofoil chord length is 70 mm, and the spanwise length is 67 mm. The hydrofoil with jet hole is shown in figure 1(a). The positions of jet holes on hydrofoil surface is 0.45C from the leading edge, and the number of jet holes is 25, the diameter of jet holes 1.4 mm. The photograph of the modified hydrofoil is shown in figure 1(b). High-speed flow field display technology is applied to study of cavitation phenomenon. The camera Sensor Array for the Sensor Array is 32 channels, 752 x 1128 pixels, memory 1 GB, and record speed of is up to 100000 fp/s. It can meet the requirements of cavitation flow field experiment with the characteristics with quick speed, small power consumption.

2.2 The measurement uncertainties

$$\sigma = \frac{P_0 - P_V}{\frac{1}{2}\rho U_0^{\ 2}} \Rightarrow \Delta\sigma = \frac{2}{\rho U_0^{\ 2}}(\Delta P_0 - \Delta P_V - \frac{2\Delta U_0}{U_0}(P_0 - P_V)) \Rightarrow \Delta\sigma_{\max} = \frac{2}{\rho U_0^{\ 2}}(|\Delta P_0| + |-\Delta P_V| + \left|-\frac{2\Delta U_0}{U_0}\right|(P_0 - P_V))$$

Table 2 shows the absolute and the relative errors in determining the cavitation number for the maximum and the minimum flow velocity, outlet pressure, and the saturation vapor pressure (which is caused by temperature changing) at 8 °angle of attack.

3 Results

The dimensionless coefficient [9] C_Q serves for a quantitative assessment of the flowrate of the controlling flow. m_{inj} is the mass flowrate of the jet. Q_{inj} *(L/h)* is the jet-flow volume flow. m_0 is the equivalent mass flowrate of liquid of the main flow that would pass through the frontal (midsection) area S_0 of the hydrofoil in case of its absence, and h is the height of the NACA0066 midsection, i.e. the section where the foil projection onto the y-axis depending on the attack angle α takes its maximum value ($h=Hmax$ at $\alpha=0°$). Q_0 is the mainstream volume flow. The injection liquid is water $\rho_{inj} = \rho_0$, so C_Q ($C_Q = \frac{m_{inj}}{m_0} = \frac{\rho_{inj} Q_{inj}}{\rho_0 U_0 S_0} = \frac{Q_{inj}}{U_0 S_0} = \frac{Q_{inj}}{U_0 ha}$) can be regarded to be approximately equal to 0.00048 Q_{inj} / U_0. L_C^{max} is the maximum length of the cavity. Table 3 shows the summary of the regimes for modified NACA0066 model considered in this study in comparison with those for the standard one. It can be seen from the table, that if the flowrate of the jet flow were different, the cavitation suppression effects are different.

For sheet cavitation, the effectiveness of the cavitation suppression is more obvious. When the cavitation number is 1.44 and the non-dimension mass flowrate coefficient is C_Q =0.0245, the cavitation suppression effectiveness is the best, and the cavity area is L_C^{max}=0.102C decreased by70.5% compared with the standard model L_{C0}^{max}=0.347C. However, when the non-dimension mass flowrate coefficient is C_Q =0, the cavity area is L_C^{max} =0.369C, increased by 6.5% compared with the standard model, which means that this structure has little influence on the shape of sheet cavitation. When the cavitation number is 1.29 and C_Q =0, the cavity length L_C^{max} =0.431C decreased by 25% compared with the standard model L_{C0}^{max}=0.572C; and when C_Q =0.0233, the cavitation suppression effectiveness is the best, in this case, the cavity area is L_C^{max} =0.275C, shortened by 52% compared with the standard hydrofoil.

When the cavitation number is reduced to 0.99, the flow field appeared unsteady intermittent cavitation phenomenon. Without jet flow (C_Q =0), the cavity area is L_C^{max}=0.964C, compared with the standard model, decreased

*Corresponding Author, Wei Wang: wangw@dlut.edu.cn

by 5.0%, which indicates that under this cavitation condition, the structure (without jet flow) has a little influence on cavitation. However, when the jet flow is entered, it can be seen that all the jet flow coefficient shows a certain degree of diminished effect on cavitation, and if the C_Q was different, the suppression effectiveness is different, and the Strouhal number (St) is also different. When C_Q=0.0202 and C_Q=0.0233, the weakening effectiveness of cloud cavitation are the best. But for C_Q=0.0202, the St number increased to 0.1743 indicating the increasing shedding frequency. While C_Q=0.0233, the corresponding Strouhal number is 0.1095, which is decreased compared with standard model. Therefore, under this condition, C_Q=0.0233 is the optimum jet flowrate coefficient. When the cavitation number is reduced to 0.83, the flow field shows strong unsteadiness. It is different from the σ=0.99, without jet flow (C_Q =0), compared with the standard model, the cavity area length L_C^{max} decreased by 8.4%, but the Strouhal number increased to 0.1633. In another word, while the maximum length of the cavity is reduced, the shedding frequency is increased. When the non-dimension mass flowrate coefficient is changed to C_Q=0.0257, the cavity area length is the minimum, and the Strouhal number is St=0.1462 also decreased compared with the standard model. The optimum jet flowrate coefficient under this condition is C_Q=0.0257.

The jet on the surface of hydrofoil can weaken or suppress cavitation, and there is an optimum mass flowrate coefficient under each working condition. On one hand, in order to get good suppress effects, the optimum mass flowrate coefficient increases with cavitation number decreasing. On the other hand, under the optimum mass flowrate coefficient, with the intensity of cavitation increasing, the effectiveness of cavitation suppression is almost liner decreased. The reason can be explained from the following aspects, smaller the cavitation number is, the cavitation becomes more severe, and during the cavity developing process, more energy is carried by the jet, so the greater the energy is needed for blocking re-entrant jet, as a result, the energy and the mass flowrate of the jet is greater. However, due to the restriction of the hydrofoil structure and the cavitation condition, the increase of momentum and energy brought by jet is smaller than that of the increase of the re-entrant jet intensity caused by the decrease of the cavitation number.

4 Conclusion

The active method for cavitation control by arranging water jet holes on the suction surface of the hydrofoil was applied to suppress cavitation. The active jet flow can completely suppress sheet cavitation, for cloud cavitation, it can weaken the development of the cavity and decrease the frequency of the shedding of the cloud cavity, but the shedding of cloud cavity cannot be avoided completely. The results also showed that under different cavitation conditions, the optimum mass flowrate coefficient is different. And the optimum mass flow coefficient increases with cavitation number decreasing. Regarding of these, this new microflow over the surface of hydrofoil can regulate the cavitating degree and show high potential of industrial application in cavitation suppression.

Figures& Tables:

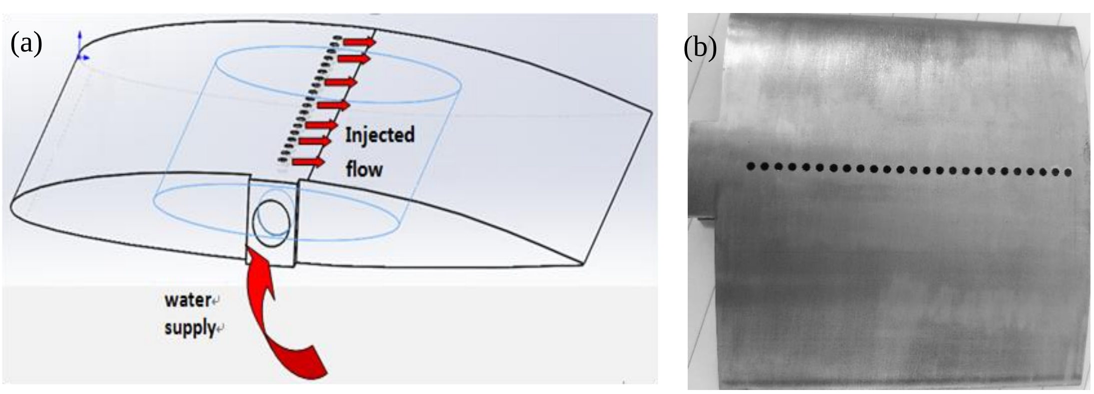

Figure 1 (a) A 3D model and (b) photograph of the modified naca0066

*Corresponding Author, Wei Wang: wangw@dlut.edu.cn

Figure 3 Instantaneous images of partial cavities (side view) of the (1) standard (without the jet holes) and modified hydrofoil model at the attack angle α = 9° for the following flow conditions: (A1) σ =1.44 standard hydrofoil sheet cavity (unmodified); (A2) σ =1.44C_Q=0.023 (sheet cavity/ subcavitating flow); (B1) σ =0.99 standard hydrofoil unsteady/cloud cavity (B2) σ =0.99 C_Q=0.023 steady cavity

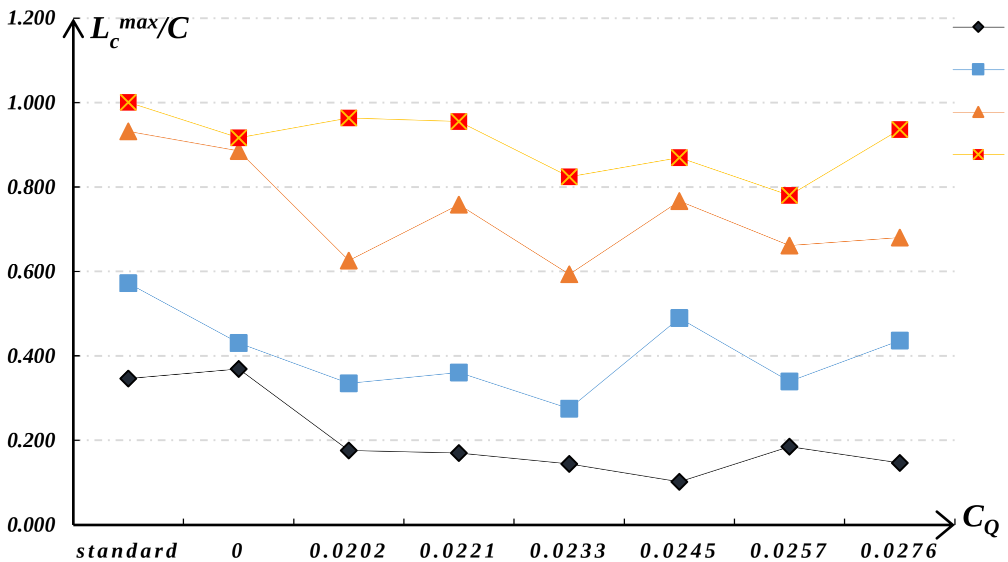

Fig 4The dimensionless length of the cavity varies with the dimensionless mass flowratecoefficient C_Q

Table 1 The basic sizes of cavitation tunnel

location	contraction	experimental section	diffuser
size	1513mm	700×70×190	1043mm

Table 2 Absolute and relative errors in determining the cavitation number

flow parameters	α=8°			
P_0/kpa	46.13	41.33	32.33	27.33

*Corresponding Author, Wei Wang: wangw@dlut.edu.cn

ΔP_0/kpa	±0.70	±0.70	±0.70	±0.70
$U_0/m \cdot s^{-1}$	7.832	7.832	7.832	7.832
$\Delta U_0/m \cdot s^{-1}$	±0.104	±0.104	±0.104	±0.104
P_v/kpa	1.94	1.94	1.94	1.94
ΔP_v/kpa	±0.192	±0.192	±0.192	±0.192
σ	1.44	1.29	0.99	0.83
$\Delta\sigma_{max}$	0.068	0.063	0.056	0.051
$\Delta\sigma_{max}/\sigma$	0.047	0.049	0.056	0.062

Table 3 Summary of the regimes for the modified NACA0066 model considered in the study in compassion with those for the unmodified one

flow conditions 8° U_0=7.832m/s		Q_{inj} (L/h)	C_Q	L_C^{max}/C	*St*
σ/regime					
1.44	transitional regime / sheet cavity	standard		0.347	Steady regimes
		0	0	0.369	
		330	0.020	0.176	
		360	0.022	0.170	
		380	0.023	0.145	
		400	0.025	0.102	
		420	0.026	0.185	
		450	0.028	0.146	
1.29	sheet cavity	standard		0.572	Steady regimes
		0	0	0.431	
		330	0.020	0.335	
		360	0.022	0.361	
		380	0.023	0.275	
		400	0.025	0.490	
		420	0.026	0.340	
		450	0.028	0.437	
0.99	unsteady intermittent cavitation	standard		0.932	0.1373
		0	0	0.886	0.1348
		330	0.020	0.626	0.1743
		360	0.022	0.758	0.1458
		380	0.023	0.594	0.1095
		400	0.025	0.766	0.1559
		420	0.026	0.661	0.142
		450	0.028	0.68	0.1345

*Corresponding Author, Wei Wang: wangw@dlut.edu.cn

0.83	cloud/ unsteady intermittent cavitation	standard		1.001	0.1511
		0	0	0.916	0.1633
		330	0.020	0.963	0.1539
		360	0.022	0.955	0.1581
		380	0.023	0.825	0.1543
		400	0.025	0.870	0.1615
		420	0.026	0.780	0.1462
		450	0.028	0.936	0.1674

References

[1] Knapp, R. T. (1955). *Recent investigations of the mechanics of cavitations and cavitation damage.* Trans Asme, 77

[2] Furness, R. A., & Hutton, S. P. (1975). *Experimental and theoretical studies of two-dimensional fixed-type cavities.* Journal of Fluids Engineering, 97(4), 515-521.

[3] Kravtsova, A. Y., Markovich, D. M., Pervunin, K. S., Timoshevskiy, M. V., & Hanjalić, K. (2013). *High-speed imaging of cavitation regimes on a round-leading-edge flat plate and naca0015 hydrofoil.* Journal of Visualization, 16(3), 181-184.

[4] Yang, J., Zhou, L., & Wang, Z. (2011). *Numerical simulation of three-dimensional cavitation around a hydrofoil.* Journal of Fluids Engineering,133(8), 081301.

[5] Li, D. Q., Grekula, M., & Lindell, P. (2010). *Towards numerical prediction of unsteady sheet cavitation on hydrofoils.* Journal of Hydrodynamics Ser B, 22(5), 741-746.

[6] Asnaghi, A. (2010). *Unsteady multiphase modeling of cavitation around naca0015.* Journal of Marine Science & Technology, 18(5), 689-696.

[7] Ganesh, H., Chang, N., & Ceccio, S. (2011). *Tip vortex cavitation suppression by mass injection.* Journal of Fluids Engineering, 233-235(5), 337-340.

[8] Timoshevskiy, M. V., Zapryagaev, I. I., Pervunin, K. S., & Markovich, D. M. (2016). *Cavitation control on a 2D hydrofoil through a continuous tangential injection of liquid: Experimental study. (Vol.1770, pp.223-256). AIP Publishing LLC*.

[9] Timoshevskiy, M. V., Zapryagaev, I. I., Pervunin, K. S., Maltsev, L. I., Markovich, D. M., & Hanjalić, K. (2017). *Manipulating cavitation by a wall jet: experiments on a 2d hydrofoil.* International Journal of Multiphase Flow.

[10] WANG, W., YI, Q., WANG,Y., LU, S., & WANG,X. (2017). *Adaptability research of hydrofoil surface water injection on cavitation suppression*. Journal of drainage and irrigation machinery engineering (JDIME), 35(6), 461-466.

[11] Wang, W., Yi, Q., Lu, S., & Wang, X. (2017). *Exploration and Research of the Impact of Hydrofoil Surface Water Injection on Cavitation Suppression*. ASME Turbo Expo 2017: Turbomachinery Technical Conference and Exposition (pp.V02DT46A013).

[12] Mäkiharju, S. A., Ganesh, H., & Ceccio, S. L. (2015). *Effect of non-condensable gas injection on cavitation dynamics of partial cavities.* Reprinted from Bacteriological Proceedings May, 656(1), 012161.

[13] Chahine, G. L., Frederick, G. F., & Bateman, R. D. (1993). *Propeller tip vortex cavitation suppression using selective polymer injection.* Journal of Fluids Engineering, 115(3), 497-503.

[14] Chang, N., Yakushiji, R., Ganesh, H., & Ceccio, S. (2009). *Mechanism and scalability of tip vortex cavitation suppression by water and polymer injection.*

[15] Kawanami, Y., Kato, H., Yamaguchi, H., Tanimura, M., & Tagaya, Y. (1997). *Mechanism and control of cloud cavitation.* Journal of Fluids Engineering, 119(4), 788-794.

[16] WANG, W., LU, S., XU, R., YI, Q., WANG,Y., & WANG,X. (2017). *Numerical study of hydrofoil surface jet flow on cavitation suppression*. Journal of drainage and irrigation machinery engineering (JDIME), 35(10), 829-834.

Acknowledgments

This work is supported by the National Basic Research Program of China (2015CB057301), and special thanks to the Collaborative Innovation on Center of Major Machine Manufacturing in Liaoning for supporting the present work.

*Corresponding Author, Wei Wang: wangw@dlut.edu.cn